

Mg II ABSORPTION IN THE SPECTRA OF HIGH AND LOW REDSHIFT QSOs

WALLACE L. W. SARGENT AND CHARLES C. STEIDEL
 Palomar Observatory, California Institute of Technology

AND

A. BOKSENBERG

Royal Greenwich Observatory

Received 1988 February 18; accepted 1988 April 28

ABSTRACT

We present a sample of 40 Mg II absorption redshifts found in the spectra of a new, uniform sample of 55 QSOs with emission redshifts in the range $1.8 \leq z_{em} \leq 3.56$ published elsewhere. The Mg II redshifts lie in the range $0.24 \leq z_{abs} \leq 1.46$. This sample is augmented by new spectra of nine QSOs with emission redshifts in the range $0.6 \leq z_{em} \leq 1.42$ which yielded one Mg II absorption system. The new data are analyzed in conjunction with samples recently published by Lanzetta, Turnshek, and Wolfe and by Tytler *et al.* In total, we have 71 Mg II absorption systems, of which 37 constitute a complete sample of independent systems with a well-defined rest equivalent width cutoff $W_0(\lambda 2796) > 0.6 \text{ \AA}$. It is found that:

1. The distribution of number of absorption systems per QSO accurately follows a Poisson distribution, as is expected for randomly distributed intervening absorbers. An application of the second Bahcall-Peebles test is also consistent with this hypothesis.

2. The density of Mg II absorption in a given observed absorption redshift range does not depend significantly on the emission redshift of the QSO.

3. The variation of Mg II system density with redshift, expressed as a power law, follows the relationship $N(z) \propto (1+z)^{1.45 \pm 0.63}$ over the redshift range $0.16 \leq z_{abs} \leq 2.14$, consistent within the errors with a constant comoving density of absorbers in a Friedmann universe with $q_0 = 0$, and possibly inconsistent if $q_0 = \frac{1}{2}$. If the results for Mg II are combined with those for C IV obtained by Sargent, Boksenberg, and Steidel, a qualitative picture emerges in which the density of absorbers increases rapidly until $z_{abs} \sim 1$, then flattens off, and finally declines beyond $z_{abs} \sim 2.5$. This is interpreted as being due to the combined effects of cosmological expansion and the chemical evolution of the absorbers.

4. There is no significant correlation of either the Mg II doublet ratio or the mean Mg II rest equivalent width with redshift.

5. The Mg II redshifts are significantly clustered on a scale $\Delta v \leq 200 \text{ km s}^{-1}$. Both the enormous amplitude of the two-point correlation function and direct observations of the absorbing galaxy imply that the apparent clustering is due to the relative motions of clouds within galaxies. There is insufficient information to say anything about clustering on larger scales.

The newly discovered Mg II redshifts significantly increase the sample available for searches for the absorbing galaxy.

Subject headings: cosmology — quasars

I. INTRODUCTION

In a recent paper (Sargent, Boksenberg, and Steidel 1988; hereinafter SBS) we obtained spectra of an unbiased sample of 55 QSOs in the redshift range $1.8 \leq z_{em} \leq 3.56$ primarily in order to study the evolution and clustering of the C IV absorbers. These same spectra also contain many low-redshift absorption systems defined by the Mg II $\lambda\lambda 2796, 2803$ doublet. In the course of the observations for the C IV survey, during periods of poor conditions, we obtained spectra of nine bright, low-redshift QSOs which add to the samples already available for Mg II absorption studies. It has been established that Mg II absorption is less common than C IV absorption (this statement will be quantified in § IV) so that it has been difficult to obtain adequate statistical samples for studying such questions as the evolution and clustering of the Mg II absorbers. In the present paper, we combine the new sample of Mg II absorption systems found in the 55 high-redshift QSOs with the results from the nine newly observed QSOs and with samples taken from the literature. Several samples of Mg II absorption redshifts are

given by Tytler *et al.* (1987). The primary sample consisted of three Mg II absorption systems, all at $z_{abs} \sim 0.4$, found in the spectra of 24 QSOs with $0.3 \leq z_{em} \leq 1.3$. Data from Foltz *et al.* (1986) and from Young, Sargent, and Boksenberg (1982; hereinafter YSB), both dealing with high-redshift QSOs, were combined with the primary sample to produce four homogeneous samples (M60, M40, M25, and M15) based on a total of 90 different QSOs. The samples are defined by the redshift intervals in which all Mg II lines of rest equivalent width $W_0 > W_{min}$ would be detected. Values of $W_{min} = 0.60, 0.40, 0.25, \text{ and } 0.15 \text{ \AA}$, respectively, were used for the four samples. A total of only 18 Mg II absorption redshifts were found in the 90 QSOs. More recently, Lanzetta, Turnshek, and Wolfe (1987; hereinafter LTW) observed a sample of QSOs (many of which were studied by YSB) at long wavelengths. As a result of our new work, we have added 41 Mg II redshifts (of which 35 are newly discovered), roughly doubling the existing samples.

Bergeron (1988) and LTW have drawn attention to the fact that the heavy-element absorption systems may be divided into

TABLE 1
Mg II $\lambda\lambda 2796, 2803$ ABSORPTION LINES

QSO	z_{em}	z_{min}	z_{max}	z_{abs}	β	$W_0(2796)$	$W_0(2803)$	QSO	z_{em}	z_{min}	z_{max}	z_{abs}	β	$W_0(2796)$	$W_0(2803)$
Q0013-004	2.086	0.38	0.76	0.4466	0.6397	0.68	0.43	Q1115+080	1.725	0.19	0.51
Q0014+818	3.377	0.91	1.49	1.1109	0.6226	0.85	0.66	Q1138+040	1.877	0.34	0.76
Q0058+019	1.959	0.29	0.72	0.6128	0.5419	1.70	1.51	Q1148-001	1.980	0.34	0.76
Q0012+030	2.810	0.70	1.15	Q1159+123	3.502	0.95	1.56
Q0114-089	3.199	0.82	1.15	Q1213+093	2.719	0.62	0.97
Q0119-046	1.937	0.29	0.65	0.6577	0.5168	0.30	0.22	Q1222+228	2.040	0.34	0.76	0.6681	0.5372	0.43	0.41
Q0142-100	2.727	0.62	1.11	0.7199	0.4893	0.27	0.19	Q1245+345	2.068	0.34	0.76
Q0150-203	2.147	0.38	0.80	0.3892	0.6738	0.50	0.32	Q1247+267	2.039	0.32	0.76
Q0151+048	1.904	0.29	0.72	0.7800	0.5152	0.36	0.21	Q1329+412	1.935	0.34	0.76
Q0207-003	2.849	0.70	1.15	Q1331+170	2.084	0.34	0.76
Q0216+080	2.990	0.73	1.16	Q1435+638	2.068	0.34	0.76
Q0226-038	2.063	0.34	0.76	1.0435	0.5602	0.44	0.47	Q1442+101	3.540	0.98	1.56
Q0229+131	2.067	0.36	0.78	1.0445	0.5599	0.31	0.16	Q1510+115	2.106	0.34	0.86
Q0237-233	2.222	0.40	1.11	Q1511+091	2.878	0.70	1.29
Q0329-255	2.689	0.70	1.15	Q1517+239	1.898	0.34	0.76	0.7382	0.4709	0.30	0.34
Q0348+061	2.060	0.39	0.81	0.3997	0.6539	0.43	0.54	Q1548+093	2.749	0.63	0.97	0.7703	0.6354	0.27	0.31
Q0421+019	2.051	0.32	0.69	Q1623+269	2.526	0.54	1.00	0.8876	0.5545	0.67	0.48
Q0424-131	2.166	0.37	0.84	0.3722	0.6664	0.34	0.21	Q1715+535	1.929	0.34	0.76	0.8885	0.5542	0.26	0.27
Q0440-168	2.679	0.70	1.15	0.4176	0.6479	0.67	0.75	Q2126-158	3.266	0.86	1.43	1.0397	0.4985	0.52	0.25
Q0449-135	3.097	0.79	1.15	Q2206-199	2.559	0.54	1.08	0.3673	0.6421	0.39	0.21
Q0450-132	2.253	0.44	0.87	Q2342+089	2.784	0.70	1.15
Q0528-250	2.765	0.70	1.15	1.0067	0.5414	1.08	1.25	Q2343+125	2.515	0.70	1.15	0.7520	0.6099	0.93	0.77
Q0831+128	2.734	0.70	1.15	1.0077	0.5411	1.07	0.88	Q2344+125	2.763	0.70	1.15	1.0169	0.5138	0.93	0.95
Q0837+109	3.326	0.88	1.54	Q2344+125	2.763	0.70	1.15	0.8380	0.6182	0.32	0.25
Q0848+163	1.925	0.27	0.72	1.4634	0.5106	0.38	0.18	Q0024+224	1.118	0.44	0.87	0.9489	0.5807	0.32	0.26
Q0848+155	2.009	0.34	0.76	1.4648	0.5102	0.49	0.34	Q0044+030	0.624	0.44	0.63
Q0852+197	2.221	0.41	0.80	0.5862	0.5455	0.44	0.38	Q0232-042	1.436	0.44	0.87
Q0854+191	1.896	0.25	0.65	0.5903	0.5437	0.38	0.27	Q0414-060	0.781	0.44	0.79
Q0913+072	2.785	0.64	0.82	Q2145+067	0.990	0.44	0.87	0.7908	0.0638	0.61	0.46
Q0958+551	1.751	0.23	0.65	0.4151	0.6764	0.35	0.30	Q2216-038	0.901	0.44	0.87
Q1017+280	1.928	0.27	0.72	Q2230+114	1.037	0.44	0.87
Q1054-034	2.114	0.36	0.76	0.2413	0.6617	0.55	0.38	Q2251+158	0.859	0.44	0.86
				Q2344+092	0.677	0.44	0.68

three categories according to their ionization state. "Low" ionization systems contain Mg II absorption, but no C IV absorption; the reverse is true for "high" ionization systems, and a third category of "mixed" systems contains both C IV and Mg II. Thus, in studying the evolution of Mg II absorbers, care must be taken not to include samples in which the Mg II absorption has been looked for in association with C IV absorption already known. Until the connections between the C IV and Mg II absorbers have been more firmly established, the Mg II systems must be treated as a separate population in order not to introduce bias into the results. However, it will be seen below that there is increasing evidence for continuity between the statistical properties of the Mg II and C IV absorbers (see also LTW).

Bergeron (1988) has shown that the absorbing galaxy can be discovered in a large proportion of cases of Mg II absorption with $z_{\text{abs}} < 0.7$. Our new sample of Mg II absorption systems will be particularly useful for further investigations of this kind, because our QSO sample is relatively faint.

In § II we describe the new observations and assemble the new Mg II samples. Statistical tests of the intervening hypothesis for the origin of the lines are applied in § III. Cosmological evolution is examined in § IV. Section V contains a discussion of the clustering of the Mg II absorbers. Our conclusions are summarized in § VI.

II. Mg II ABSORPTION SAMPLES

a) Observations

Table 1 contains a list of the 55 QSOs observed by SBS. For each object, we give in column (2) the emission redshift and in columns (3) and (4) the minimum and maximum redshifts over which Mg II absorption could have been found. The spectra used by SBS were obtained with the University College London IPCS detector mounted on the blue camera of the double spectrograph at the Cassegrain focus of the Hale 5.08 m telescope. The resolution was 1.5 \AA or 0.7 \AA and the spectra generally cover the wavelength region from slightly longward of the C IV $\lambda 1549$ emission line down to the Ly α emission line. Care was taken to obtain a uniform signal-to-noise (S/N) ratio of ~ 20 . Complete details on the calibration and reduction of the spectra, and on the method used for selecting and identifying the absorption lines, are given in § II of SBS. The resulting Mg II redshifts are listed in column (5) of our Table 1. Details of other lines, particularly those of Fe II, are given in Table 3 of SBS; plots of the original spectra are shown in Figure 1 of SBS. In column (6) we give the apparent "ejection" velocity relative to the emission redshift of the QSO in terms of the fraction of the speed of light β . This is calculated from the expression

$$\beta = \frac{(1 + z_{\text{em}})^2 - (1 + z_{\text{abs}})^2}{(1 + z_{\text{em}})^2 + (1 + z_{\text{abs}})^2}. \quad (1)$$

(It will be seen that values of β in the range 0.5 to 0.6 are common; the highest value is $\beta = 0.677$ in Q0854 + 191. We have eschewed searching for Mg II absorption in the Lyman α forest, hence the lack of even higher values of β .) The last two columns of Table 1 list the rest equivalent widths of the two Mg II lines.

Additional observations of the nine low-redshift QSOs listed in Table 2 were made using a setup identical to that employed by SBS. These observations were made on the night of 1984 November 2/3 during conditions of exceptionally poor seeing and bright moonlight which made it impossible to continue the

TABLE 2
LOW REDSHIFT OBSERVATIONS

Object	z_{em}	Date (UT)	FWHM (\AA)	λ Range (\AA)	Exposure (s)
Q0024 + 224.....	1.118	1984 Nov 2	1.5	4040–5240	5000
Q0044 + 030.....	0.624	1984 Nov 3	1.5	4040–5240	4000
Q0232 – 042.....	1.436	1984 Nov 3	1.5	4040–5240	4000
Q0414 – 060.....	0.781	1984 Nov 3	1.5	4040–5240	4000
Q2145 + 067.....	0.990	1984 Nov 2	1.5	4040–5240	3000
Q2216 – 038.....	0.901	1984 Nov 2	1.5	4040–5240	5000
Q2230 + 114.....	1.037	1984 Nov 3	1.5	4040–5240	6000
Q2251 + 158.....	0.859	1984 Nov 2	1.5	4040–5240	4000
Q2344 + 092.....	0.677	1984 Nov 3	1.5	4040–5240	3000

regular SBS program. We used a fixed wavelength range for these observations, independent of the redshift of the QSO. Consequently, the Mg II $\lambda 2800$ emission line falls at various places in the observed spectral window; for the five QSOs with $z_{\text{em}} \geq 0.87$, the Mg II emission was outside the observed range. The spectra were reduced using the standard methods detailed in SBS. Plots of the resulting spectra are shown in Figure 1. The spectra were searched for absorption lines using the methods described in SBS. The results are shown in Table 3. Only one Mg II absorption redshift was found in the nine QSOs. It is listed along with information on the observed redshift windows for all nine objects at the bottom of Table 1.

b) Samples

We have used our data alone, and also combined our data with samples taken from the literature, as described in § I, to produce five samples of Mg II absorption systems. They are referred to as samples MG0–MG 4 and are listed in Table 4. Sample MG 1 contains all 37 Mg II redshifts from our data for which the rest equivalent width of the $\lambda 2796$ line $W_0(2796) > 0.3 \text{ \AA}$. Lines of this strength could have been detected in all of the spectra. In order to be consistent with previous workers, we require no specific strength for the $\lambda 2803$ component of the doublet, although it must have satisfied the stringent $5 \sigma(W)$ line acceptance criterion used in SBS and in the present paper. In general, because of the lower S/N ratio of their spectra, the other authors have used a cutoff of $W_0(2796) > 0.6 \text{ \AA}$. We define a corresponding sample MG 2 which contains 17 redshifts. Since the LTW observations, like ours, were mainly of high-redshift QSOs, we have defined an amalgamated sample MG 3 containing 33 redshifts with $W_0(2796) > 0.6 \text{ \AA}$. (We note that several of the QSOs observed by LTW were the same ones observed by SBS, but at longer wavelengths. There was no overlap in the wavelength regions observed, so that for these QSOs there are two independent observed redshift ranges.) Finally, we define a sample MG 4 which contains the 41 red-

TABLE 3
ABSORPTION LINES*

No.	λ_{obs}	$\sigma(\lambda)$	W_{obs}	$\sigma(W)$	S/N	ID	z_{abs}
Q2145 + 067							
1.....	5008.09	0.17	1.10	0.06	41.1	Mg II(2796)	0.7909
2.....	5020.36	0.16	0.82	0.06	38.8	Mg II(2803)	0.7907

* No lines were found in the spectra of the QSOs Q0024 + 224, Q0044 + 030, Q0232 – 042, Q0414 – 060, Q2216 – 038, Q2230 + 114, Q2251 + 158, and Q2344 + 092.

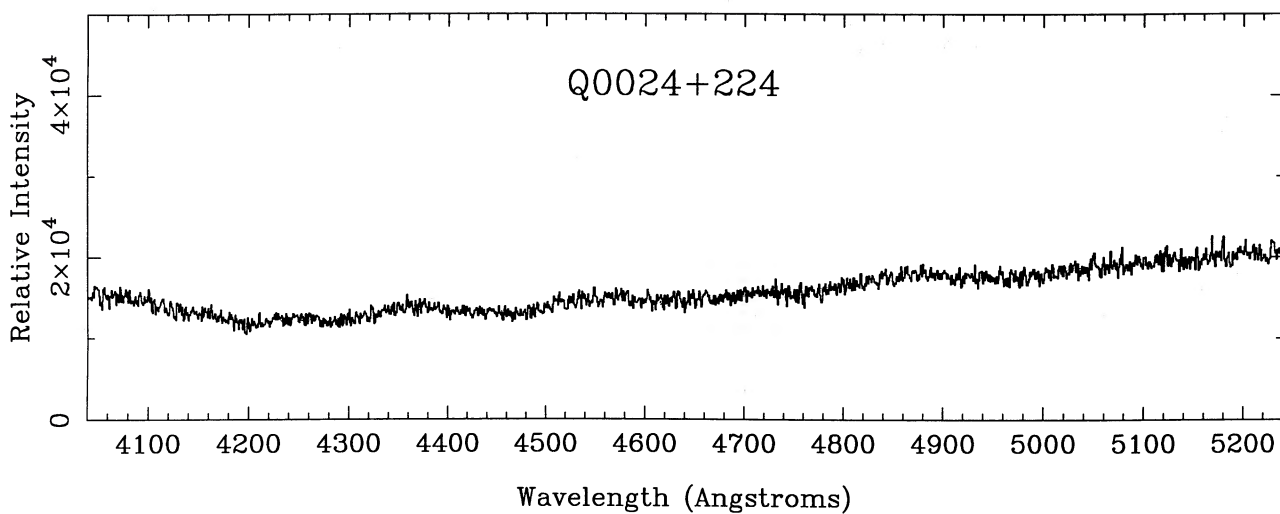


FIG. 1a

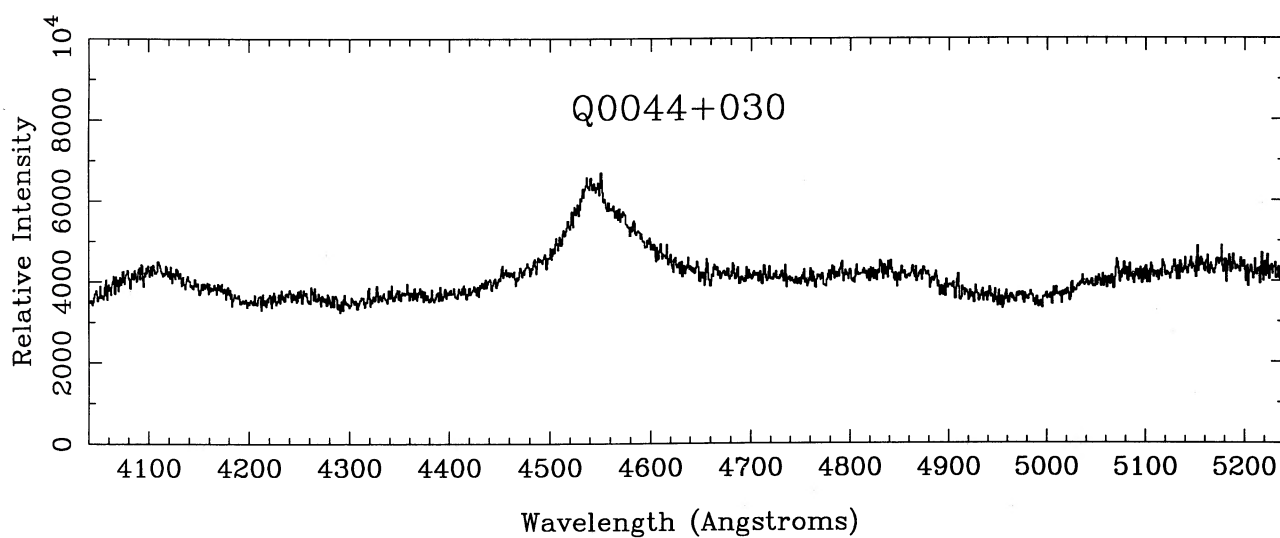


FIG. 1b

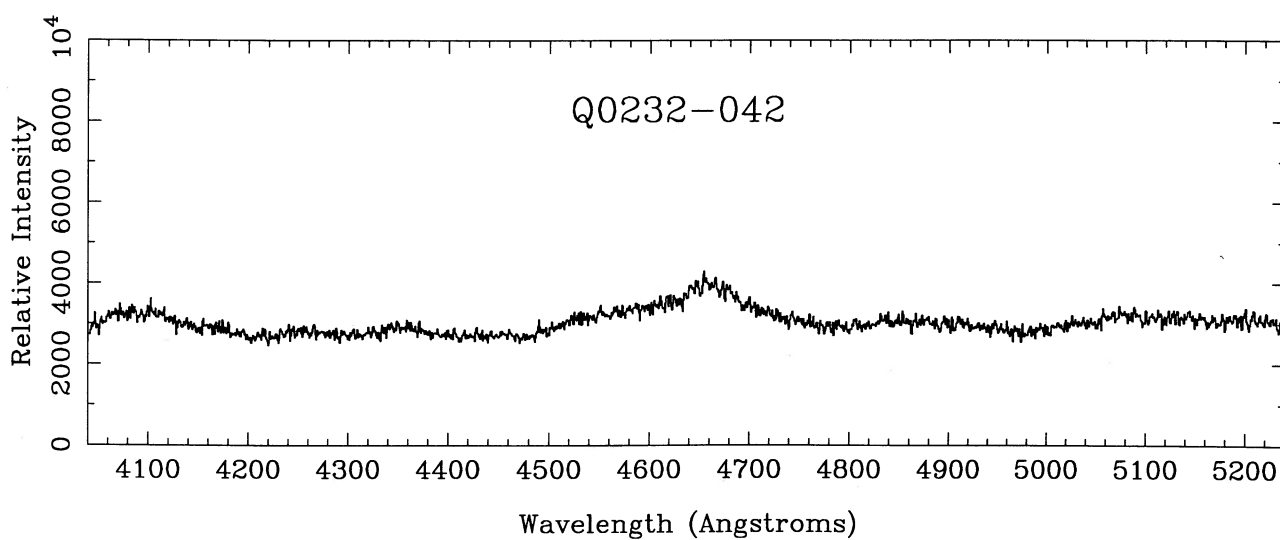


FIG. 1c

FIG. 1.—Plots of the spectra for the nine newly observed low-redshift QSOs. Measurements for the indicated absorption lines are given in Table 3.

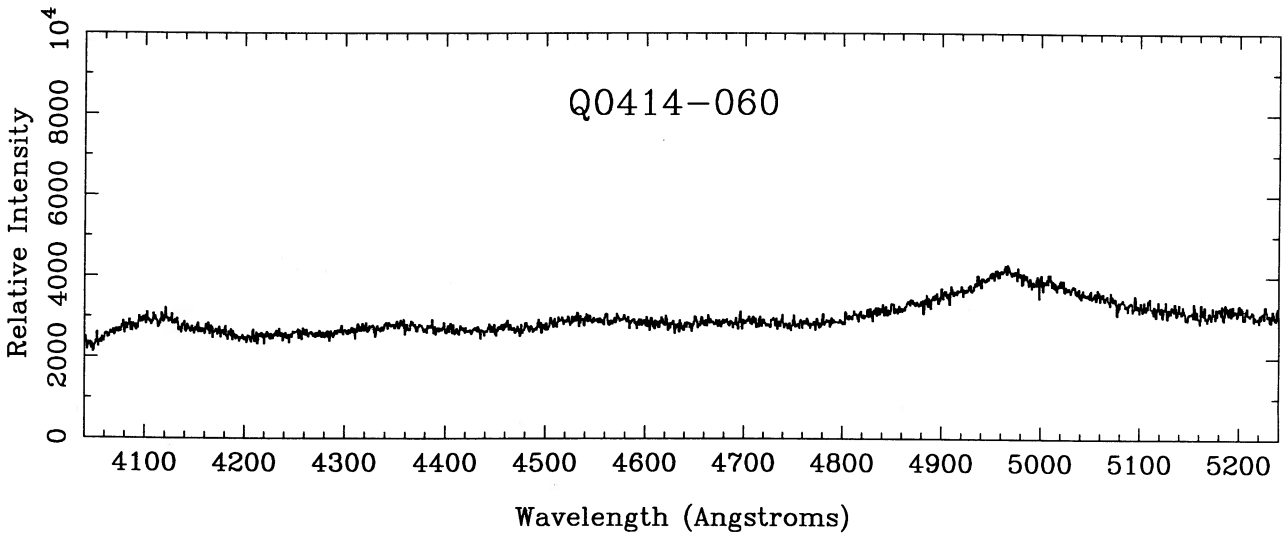


FIG. 1d

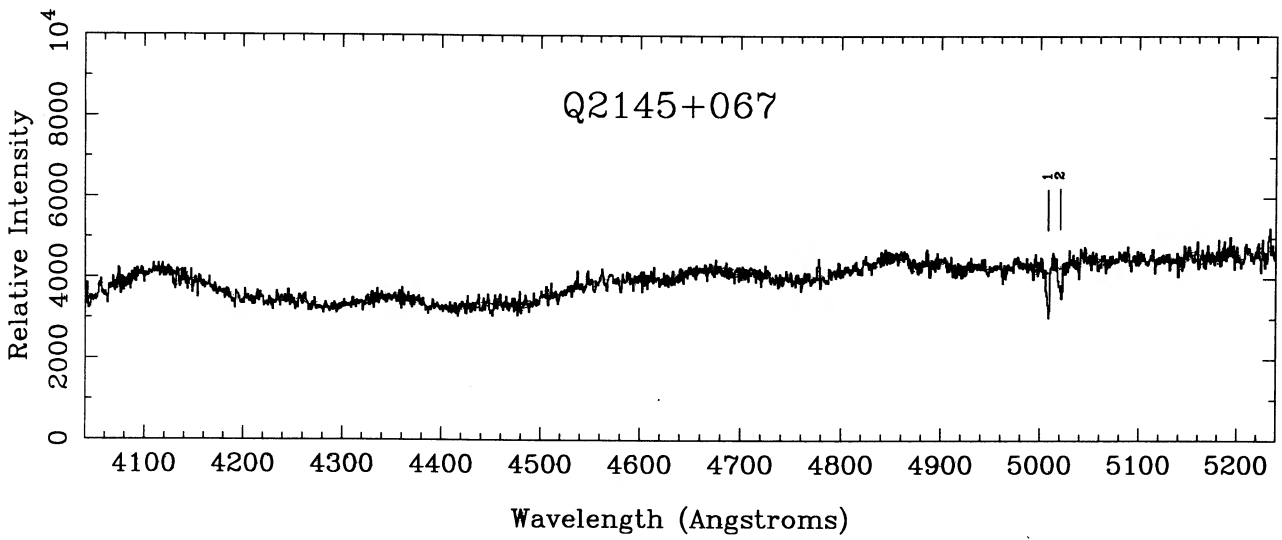


FIG. 1e

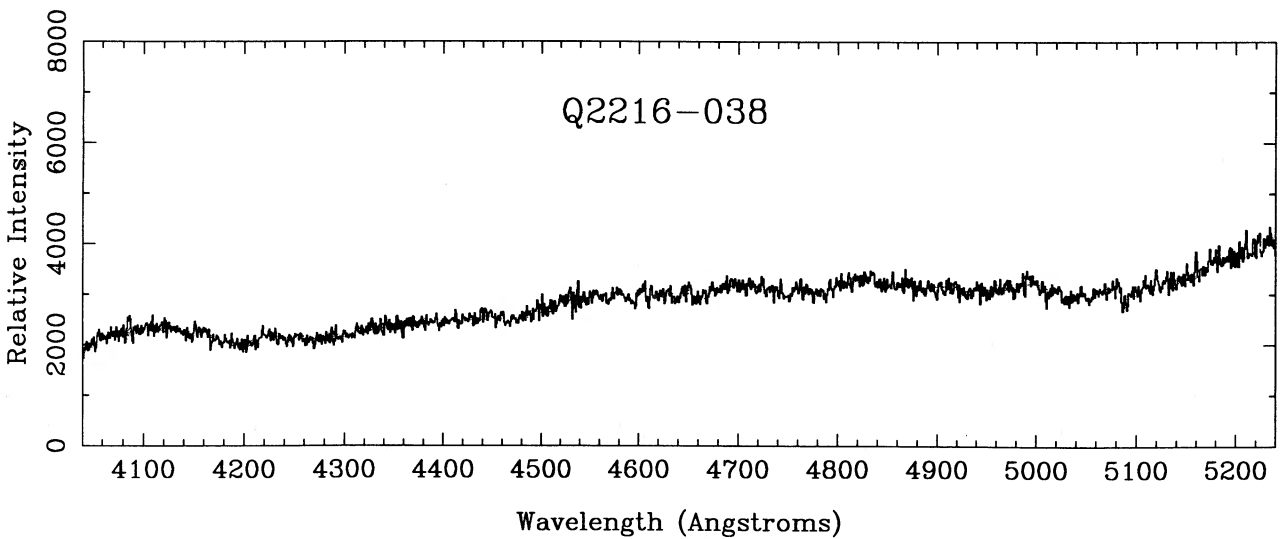


FIG. 1f

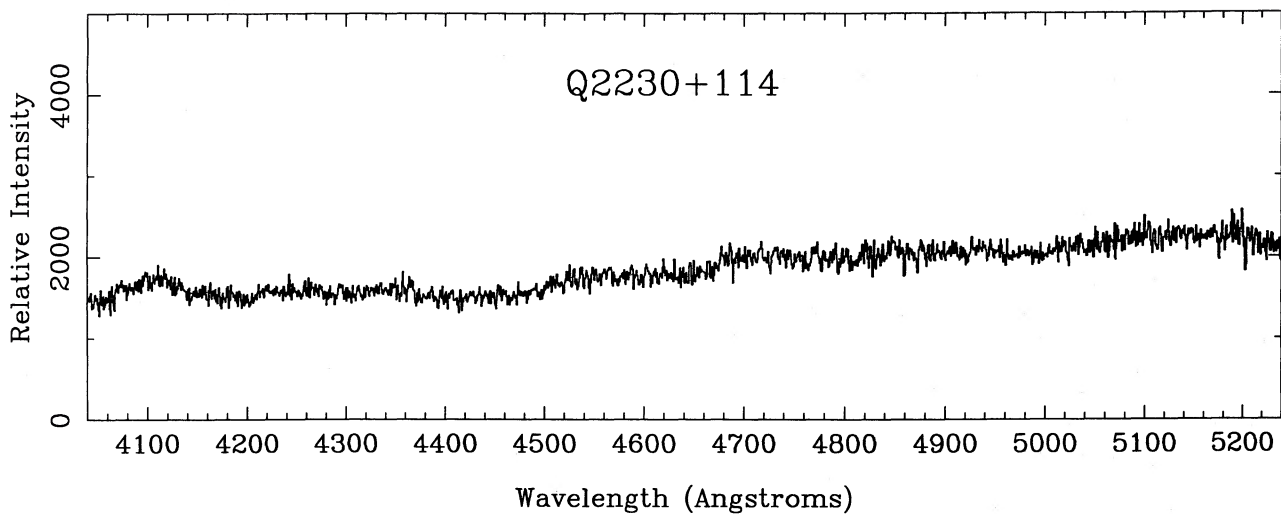


FIG. 1g

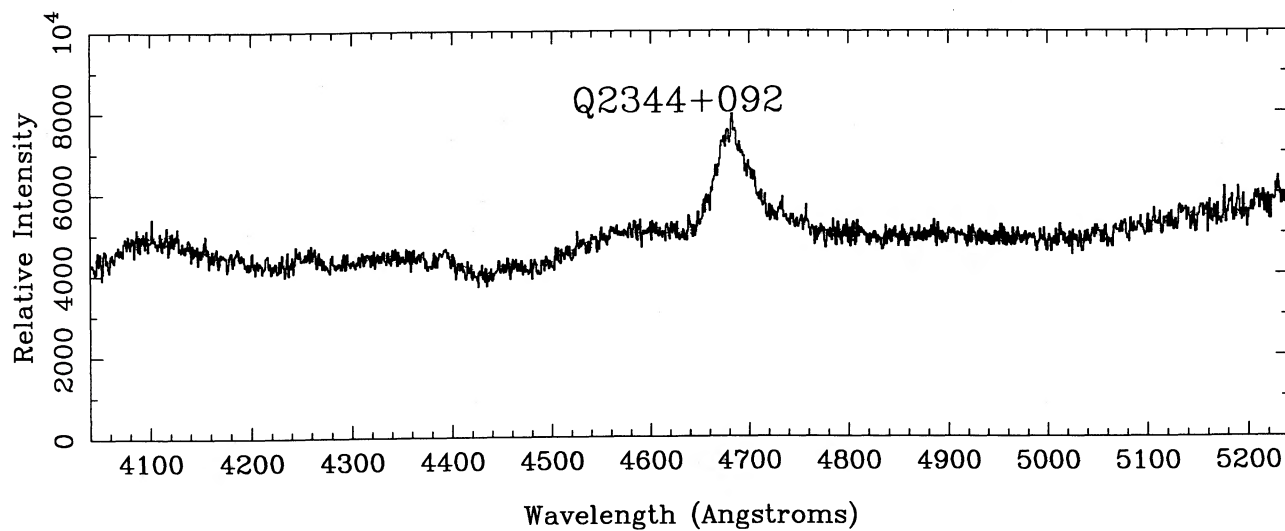


FIG. 1h

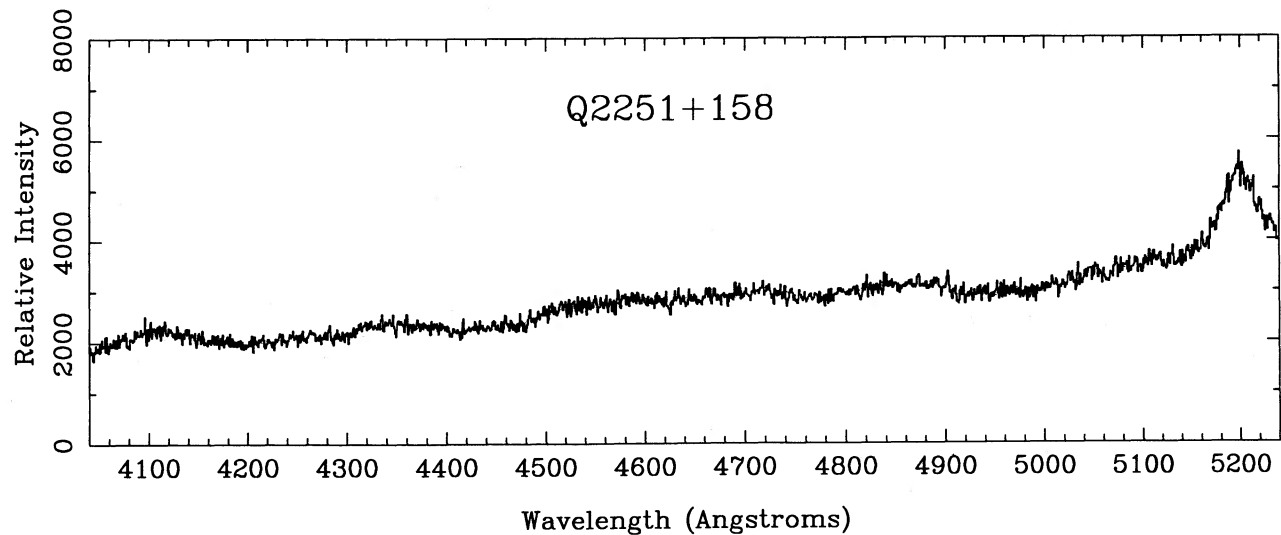


FIG. 1i

TABLE 4
THE Mg II ABSORPTION SYSTEM SAMPLES

Criteria	Sample	Number	W_*	$\sigma(W_*)$	N_*	$\sigma(N_*)$
All included	MG 0	41	0.66	0.14	1.52	0.25
$W_0(\lambda 2796) > 0.3$	MG 1	37	0.55	0.10	2.34	0.46
$W_0(\lambda 2796) > 0.6$	MG 2	17	0.67	0.58	1.51	1.21
$W_0(\lambda 2796) > 0.6 + \text{LTW}$	MG 3	34	0.77	0.26	1.55	0.48
$W_0(\lambda 2796) > 0.6 + \text{LTW} + \text{Tytler } et \text{ al.}$	MG 4	41	0.84	0.20	1.23	0.28

shifts with $W_0(2796) > 0.6 \text{ \AA}$ in the combined lists of LTW, Tytler *et al.*, and the present paper. Statistical properties of the foregoing samples are listed in Table 4.

A glance at Table 1 reveals several cases in which two Mg II systems are found in the same QSO with separations $\Delta z \sim 0.0010$. The systems in these closely spaced pairs are clearly associated and should not be counted separately for many statistical purposes. For this reason, as in SBS, we have defined "Poisson" samples P0–P4, equivalent to the samples MG 0–MG 4 defined above, except that systems in the same object with separations $\Delta v < 1000 \text{ km s}^{-1}$ were counted as one. Properties of the Poisson samples are summarized in Table 5.

In the following two sections, we use the samples defined in Tables 4 and 5 to investigate statistics of the evolution and clustering of the Mg II absorption systems.

III. TESTS OF THE INTERVENING HYPOTHESIS

The intervening hypothesis for the origin of QSO absorption lines makes a very strong prediction that the distribution of the number of absorption systems per QSO should be a Poisson distribution, provided the individual spectra cover the same redshift range Δz . If we take the Poisson sample P1 we find 31 unassociated redshifts for which $W_0(2796) > 0.3 \text{ \AA}$ in the 55 high-redshift QSOs of SBS plus the nine additional low-redshift QSOs. Thus the mean number of redshifts per QSO is $\lambda_c = 0.484$. The predictions of a Poisson distribution as compared with the observed numbers are shown in Table 6. The results of a χ^2 test summarized in column (4) of Table 6 show that the agreement with a Poisson distribution is excellent.

A more sophisticated version of the test is to allow for the different redshift coverages Δz_i of the spectra (but not for any possible evolution in the mean density of absorbers with redshift). Formulae for the appropriate likelihood function f and for its variance are given in equations (16), (17), and (18) of YSB. On applying the test to sample P1, we find

$$\ln f = -57.20 \quad (2)$$

$$\langle \ln f \rangle = -57.59 \quad (3)$$

$$\sigma(\ln f) = 8.46, \quad (4)$$

TABLE 5
THE "POISSON" SAMPLES

Sample	Number	$\langle z_{\text{abs}} \rangle$	N^a	$\sigma(N)$	γ^b	$\sigma(\gamma)$
P0	34	0.726	1.24	0.21	-0.29	1.15
P1	31	0.732	1.13	0.20	-0.16	1.20
P2	14	0.770	0.51	0.12	1.02	1.74
P3	30	1.236	0.63	0.10	1.09	0.88
P4	37	1.116	0.54	0.08	1.45	0.63

^a Mean number density of absorption systems per unit redshift interval.

^b Maximum likelihood estimation assuming the form $N(z) \propto (1+z)^\gamma$.

again showing very good agreement with a Poisson distribution.

The second test of Bahcall and Peebles (1969) examines the uniformity of the spatial distribution of absorbers over the observed range of redshift, taking into account cosmological effects and assuming that their comoving density does not evolve in cosmic time. Again, the appropriate formulae are given in YSB. The result of applying a Kolmogorov-Smirnov (K-S) test for sample P1 is that

$$D_{\text{max}} = 0.198, \quad P(D > D_{\text{max}}) = 0.176 \quad (q_0 = \frac{1}{2}) \quad (5)$$

$$D_{\text{max}} = 0.206, \quad P(D > D_{\text{max}}) = 0.143 \quad (q_0 = 0), \quad (6)$$

where D_{max} is the maximum deviation of the observed cumulative distribution function from that of a flat distribution and $P(D > D_{\text{max}})$ is the probability of obtaining a value of D_{max} greater than the observed value if the sample is randomly drawn from the flat distribution. Thus, for both values of q_0 , the observed distributions do not differ significantly from a flat distribution and therefore the data are again consistent with what would be expected for cosmologically distributed intervening absorbers.

IV. EVOLUTION IN REDSHIFT

a) Evolution in Number Density

The number density of absorption systems of a given column density is expected, in a simple Friedmann universe, to depend on redshift according to the expression (see SBS for references)

$$dN/dz \equiv N(z) = N_0(1+z)(1+2q_0z)^{-1/2}, \quad (7)$$

where $N_0 = (c/H_0)\Phi_0 \pi r_0^2$ is the local density at zero redshift. Following Sargent *et al.* (1980; hereinafter SYBT), we express the observed redshift dependence by a power law $N(z) \propto (1+z)^\gamma$, where $\gamma = 1$ ($q_0 = 0$) and $\gamma = \frac{1}{2}$ ($q_0 = \frac{1}{2}$). In SBS, it was shown that for the more numerous C IV absorption systems, $\gamma = -1.2 \pm 0.7$ over the redshift range $1.3 \leq z_{\text{abs}} \leq 3.4$. Thus, at high redshifts, the density of these heavy element absorption systems actually *decreases* with increasing redshift; this was attributed to the effects of early nucleosynthesis in the

TABLE 6
BAHCALL-PEEBLES TEST 1 (UNCORRECTED)^a

Number of Systems	Expected QSOs	Observed QSOs	χ^2
0	39.4	39	0.0
1	19.1	20	0.1
2	3.1	4	0.3
3	0.4	1	0.9
Total	64.0	64	1.3

^a Using sample P1, assuming that the observed redshift interval Δz is the same for each of the QSOs.

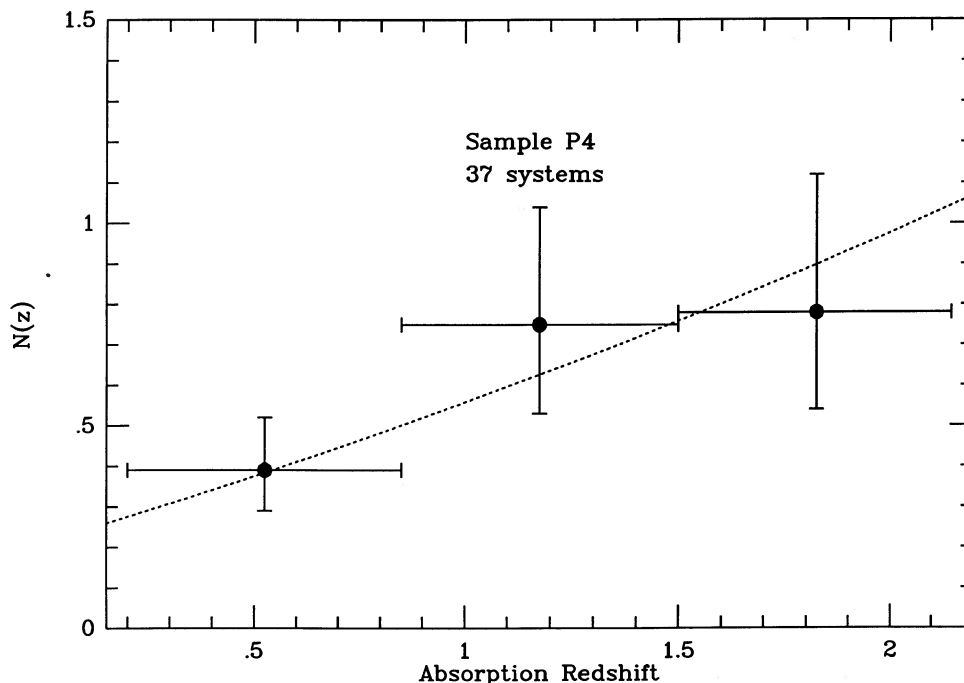


FIG. 2.—Plot of the binned number of Mg II absorption systems per unit redshift interval $N(z)$ for sample P4. The dotted curve is a result of the maximum likelihood fit assuming the form $N(z) \propto (1+z)^\gamma$. Here $\gamma = 1.45$ (see Table 5).

absorbers. The paucity of Mg II absorption systems, together with the small redshift range over which they were observed, has made published determinations of γ very unreliable. Thus, Tytler *et al.* (1987) found $\gamma = 3.5 \pm 2.2$ over the range $0.16 \leq z_{\text{abs}} \leq 1.37$. Adding their data to those of Tytler *et al.*, LTW found a more accurate slope, namely $\gamma = 2.4 \pm 0.8$. This was calculated for a sample containing redshifts in the range $0.16 \leq z_{\text{abs}} \leq 2.14$ and with $W_0(2796) > 0.6 \text{ \AA}$. Thus, LTW found clear evidence for cosmological evolution in the density of Mg II absorbers in the sense that the product of the effective radius and the number density of the absorbers is greater at larger redshifts. This effect is established at the 2.4σ level for $q_0 = \frac{1}{2}$ and at the 1.8σ level for $q_0 = 0$. A plot of $N(z)$ versus absorption redshift for our amalgamated sample (P4) is shown in Figure 2. A maximum likelihood fit of a power-law dependence yields $\gamma = 1.45 \pm 0.63$. This is consistent with no evolution in the properties of the absorbers if $q_0 = 0$, and inconsistent at only the 1.5σ level if $q_0 = \frac{1}{2}$. Note that our new absorption system sample fills in the “gap” in redshift between the samples of Tytler *et al.* and LTW. An examination of Figure 2 suggests that a power-law fit may not be the correct representation of the data points. Instead, one has the impression that there may be a steep rise in $N(z)$ up to $z \sim 1$, followed by a distinct flattening in the distribution. This can only be resolved by the acquisition of much larger samples of Mg II redshifts. However, we recall from SBS that the number density of C IV redshifts is at most flat, and possibly falling, with increasing redshift in the range $1.3 < z_{\text{abs}} < 3.4$. It is entirely possible that both the Mg II and C IV system densities rise rapidly up to $z \sim 1$, then flatten off between $z \sim 1$ and $z \sim 2.5$, and fall at higher redshifts. Certainly, the presently available data do not necessarily imply that the evolution of C IV is qualitatively different from that of Mg II. Observations with the Hubble Space Telescope will enable the evolution of

C IV systems to be directly compared with that for Mg II systems at redshifts $z_{\text{abs}} < 1$.

Although it is true that the general density of C IV systems exceeds that of Mg II systems, there is growing evidence that this is largely an effect of the different redshift ranges accessible in the two ions. We observe that, in the redshift range $1.3 < z_{\text{abs}} < 2$ in which the densities can be compared directly, for $W_0 > 0.6 \text{ \AA}$, $N = 1.02 \pm 0.17$ for C IV, and $N = 0.80 \pm 0.04$ for Mg II (sample P4). It is also useful to calculate the effective cross sectional radius for absorption R_* for a fiducial L_* galaxy, assuming that the galaxian luminosity function follows a Schechter (1976) function and that radius scales with luminosity as $R \propto L^{5/12}$. (See SBS for a discussion of the likely validity of these assumptions.) The results of calculations of R_* for different C IV samples (taken from SBS) and for our Mg II samples are shown in Table 8. We observe that, for Mg II and C IV samples with comparable rest equivalent width cutoffs, the values of R_* are very similar.

There is a natural explanation of the qualitative behavior of the evolution of heavy-element redshift systems obtained by “patching together” the Mg II systems at low redshifts and the C IV systems at high redshifts. The rise in $N(z)$ at low redshifts would be due to the expansion of the universe, and the fall at high redshifts would be due to a systematic decrease in heavy element abundance. Figure 2 gives a hint that the rise in $N(z)$ at small redshifts might be too steep to be compatible with $q_0 = \frac{1}{2}$ ($\gamma = 0.5$). It would be extremely useful to obtain more data for low-redshift Mg II absorption systems so that this trend might be examined more carefully.

b) Equivalent Width Distribution

Tytler *et al.* (1987) found that the number density of Mg II absorption systems as a function of rest equivalent width

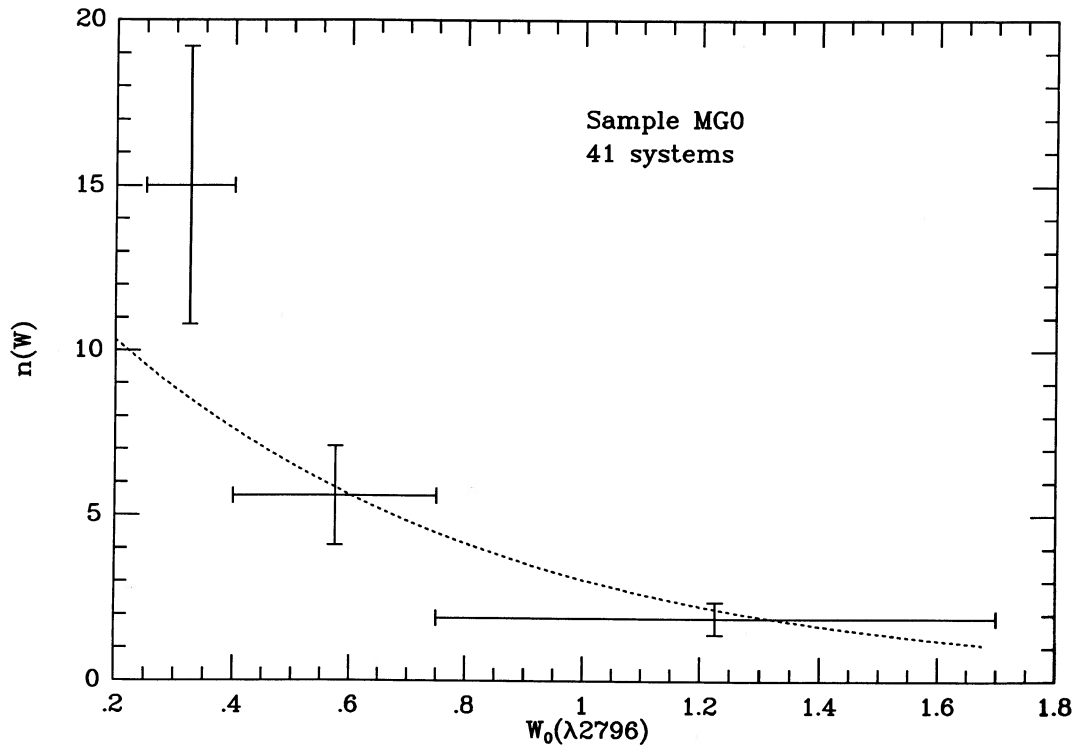


FIG. 3.—Plot of the binned distribution of equivalent width for the Mg II $\lambda 2796$ lines in sample MG 0. The dotted curve is the result of a maximum likelihood fit to the data using the exponential form $n(W) \propto \exp(-W/W_*)$. Here $W_* = 0.66$ (see Table 4).

$W_0(\lambda 2796)$ could be represented by a power law

$$n(W) = (AW_0)^{-2.1} \quad (8)$$

for $W_0 \geq 0.25 \text{ \AA}$, where $A = 0.11 \pm 0.03$. LTW found a somewhat better fit using an exponential distribution, first used for the Ly α forest lines by SYBT,

$$n(W) = \left(\frac{N_*}{W_*}\right) \exp\left(-\frac{W}{W_*}\right), \quad (9)$$

where $N_* = 1.76 \pm 0.40$ and $W_* = 0.88 \pm 0.19$ at a mean redshift $\langle z_{\text{abs}} \rangle = 1.62$. With our enhanced data sample MG 0, we find $N_* = 1.52 \pm 0.25$ and $W_* = 0.66 \pm 0.14$ at a mean redshift of $\langle z_{\text{abs}} \rangle = 0.726$. Given the rather large difference in mean absorption redshifts for the two samples, there is no evidence for any significant evolution in the equivalent width distribution with redshift. The fit to our data is shown in Figure 3. As was found for the C IV lines in SBS, and as has been found in

general for the lines of the Ly α forest, there are more weak Mg II lines than would be predicted based on the assumed exponential distribution. This discrepancy was not obvious from the data of LTW because the rest equivalent width cutoff was generally larger.

Tytler *et al.* (1987) found a positive correlation between $W_0(2796)$ and redshift z which was significant at the 90%–95% confidence level from 14 low-redshift Mg II systems. On the other hand, LTW found no significant correlation with a somewhat larger sample which extended over a larger redshift range. We have used the Spearman and Kendall rank correlation tests to look for such an effect using samples MG 1 and MG 4. There is no significant correlation between the two quantities for either of the samples; the complete results of the two tests are summarized in Table 7.

Clear evidence for a systematic increase in the doublet ratio with redshift was found by SBS from their very large C IV sample. Again using samples MG 1 and MG 4, we have

TABLE 7
RESULTS OF RANK CORRELATION TESTS

Test Variables	Sample	ρ_s^a	$(\rho_s/\sigma)^b$	S_s^c	ρ_k^d	$(\rho_k/\sigma)^e$	S_k^f
$W_0(2796), z_{\text{abs}}$	MG 1	0.147	0.385	0.582	0.090	0.785	0.433
$W_0(2796), z_{\text{abs}}$	MG 4	0.099	0.536	0.629	0.049	0.449	0.653
DR, z_{abs}	MG 1	-0.158	0.850	0.389	-0.130	1.040	0.296
DR, z_{abs}	MG 4	-0.015	0.090	0.927	-0.038	0.339	0.734

^a Spearman rank correlation coefficient.

^b Number of standard deviations from the null hypothesis (no correlation) for the Spearman test.

^c Significance level of the deviation for the Spearman test.

^d Kendall rank correlation coefficient.

^e Number of standard deviations from the null hypothesis (no correlation) for the Kendall test.

^f Significance level of the deviation for the Kendall test.

TABLE 8
VALUES OF R_* (h^{-1} kpc)

Sample ^a	$(L/L_*) > 0^b$	$(L/L_*) > 0^b$	$(L/L_*) > 0.5^c$	$(L/L_*) > 0.5^c$
	$q_0 = 0$	$q_0 = \frac{1}{2}$	$q_0 = 0$	$q_0 = \frac{1}{2}$
S1	56.7	74.9	93.0	122.8
S2	55.0	72.1	90.2	118.2
S3	44.5	58.4	73.0	95.8
S4	43.4	56.5	71.2	92.7
S5	42.9	55.5	70.4	91.0
P0	50.0	57.3	82.0	94.0
P1	47.7	54.7	78.2	89.7
P2	31.6	36.5	51.8	59.9
P3	31.3	38.3	51.3	59.9
P4	29.8	35.9	48.9	58.9

^a Samples having the prefix "S" are C IV samples from SBS.

^b Assumes a Schechter luminosity function, and that galaxies of all luminosities contribute to the absorption cross section. (See SBS for details of the calculation.)

^c Assumes a truncated Schechter luminosity function, so that only galaxies brighter than $0.5L_*$ contribute to the absorption cross section.

applied Spearman and Kendall tests and find no correlation between the Mg II doublet ratio and redshift. The quantitative results are summarized in Table 7. The Mg II systems in these samples are at significantly lower redshifts than the C IV data for which evolution of the doublet ratio was found; consequently, it is not surprising that we find no evidence for evolution of the doublet ratio with redshift under the hypothesis that such evolution is due to early chemical enrichment of the absorbers.

c) Dependence on Emission Redshift

It is a common experience of workers in the field that Mg II absorption in the spectra of low-redshift QSOs is rare. On the other hand, there is a suspicion that Mg II absorption is more common in the spectra of high-redshift QSOs, which have been studied primarily for C IV absorption. Although this suspicion was voiced by Perry, Burbidge, and Burbidge (1978), it was contradicted by Weymann *et al.* (1979), but only on the basis of a sample containing five Mg II systems. A more stringent statistical test by Tytler *et al.* also found no evidence for an association between Mg II systems and the redshifts of the QSOs in which they are observed. It is clearly important to test these impressions objectively, because if there is an association, then the absorption cannot be due to cosmologically distributed intervening objects.

We found above that the number density of Mg II absorption systems rises rapidly up to a redshift $z_{\text{abs}} \sim 1$; therefore, it is important that tests for a difference in density between high and low-emission redshift QSOs be conducted over the same restricted range in z_{abs} . For sample P4, we find a mean density of Mg II systems with $z_{\text{abs}} \leq 0.90$ of $N = 0.32 \pm 0.15$ for the 36 QSOs with $z_{\text{em}} < 1.5$, and $N = 0.42 \pm 0.13$ for the 103 QSOs with $z_{\text{em}} > 1.5$. On changing the absorption redshift limit to $z_{\text{abs}} \leq 0.60$, we find $N = 0.30 \pm 0.14$ ($z_{\text{em}} < 1.5$) and $N = 0.22 \pm 0.08$ ($z_{\text{em}} > 1.5$). Thus, the density of Mg II systems is statistically the same in QSOs with high and low-emission redshifts, respectively. This again supports an intervening origin for the absorption systems.

V. CLUSTERING

Because of the general paucity of Mg II systems, information on clustering is practically nonexistent. However, some cases of

multiple structure in Mg II absorption are known. Thus, Boksenberg, Carswell, and Sargent (1979) found four velocity components spread over $\Delta v = 165 \text{ km s}^{-1}$ in the $z_{\text{abs}} = 0.424$ Mg II system in the spectrum of Q0753+178; Bergeron, D'Odorico, and Kunth (1987) found six components spread over $\Delta v = 560 \text{ km s}^{-1}$ in the $z_{\text{abs}} = 0.8526$ redshift system in Q1327-206; the $z_{\text{abs}} = 0.524$ system in the spectrum of A0235+164 shows many components over a velocity range of $\Delta v \sim 350 \text{ km s}^{-1}$ (Crotts 1987). As Blades (1988) has pointed out, the velocity structures present in these Mg II systems are different from those seen in our Galaxy, or those seen in the line of sight to the supernova 1987A in the LMC. York *et al.* (1986) have proposed that complex Mg II absorption can be produced in starburst galaxies; as Blades points out, the galaxies identified as Mg II absorbers (Bergeron 1988) often show evidence for high star-formation rates.

We remarked in § II that there is a clear excess of Mg II systems in the same QSO with separations $\Delta z \sim 0.0010$ (we constructed the Poisson samples for this very reason). Using the techniques detailed in § VII of SBS, we have calculated the two-point correlation function for the Mg II systems in sample MG 0. (Since we are interested in clustering on small scales, it is possible to use all of the data.) The results are shown in Figure 4. As expected, there is a pronounced peak in the correlation function near the origin, on scales $\Delta v \leq 200 \text{ km s}^{-1}$. The paucity of Mg II systems makes it very difficult to determine the background level in the two-point correlation function; there are only four QSOs with widely separated pairs of systems, and one with a widely separated triple. The total number of "background" splittings is seven spread over a velocity range of roughly $40,000 \text{ km s}^{-1}$. The background level per 50 km s^{-1} bin in Figure 4 is ~ 0.03 . Therefore, the correlation peak near the origin is highly significant. Using our very rough estimate of the background, the amplitude of the observed correlation on scales $100 < \Delta v < 200 \text{ km s}^{-1}$ is ~ 80 . The corresponding amplitude for the C IV sample A1 from SBS is ~ 10 . Thus, it appears that the Mg II redshifts are much more strongly clustered on these small velocity scales than the C IV systems; however, it may be that we have seriously underestimated the background level for the Mg II two-point correlation function. Many more Mg II splittings must be observed before any definite conclusions can be reached concerning the significance of the difference between the C IV and Mg II correlation functions on these small velocity scales. On the other hand, at present we can say nothing about Mg II clustering on larger scales. In particular, we showed in SBS that only splittings on scales $\Delta v \geq 200 \text{ km s}^{-1}$ could be unambiguously attributed to galaxy-galaxy clustering. Therefore the clustering that we have observed could be due to relative motions of clouds within galaxies. Direct evidence that this is the case is provided by Bergeron's (1988) result that single, luminous galaxies associated with Mg II absorption redshifts are found close to 80% of the QSOs that she studied. Note that even if the clustering on scales $200 \leq \Delta v \leq 600 \text{ km s}^{-1}$ found by SBS for their C IV sample were also present in the Mg II sample, it would not be detected.

Tytler *et al.* (1987) noted that 10 out of their 14 Mg II systems in a complete sample occurred in five pairs of two systems per QSO. The velocity separations in this case were relatively large, namely $\Delta v = 11,038 \text{ km s}^{-1}$ in Q0119-046, $30,005 \text{ km s}^{-1}$ in Q0453-423, 1816 km s^{-1} in Q0454-220, 355 km s^{-1} in Q0843+136, and $46,630 \text{ km s}^{-1}$ in Q1209+107. Tytler *et al.* show that the probability of observing five or more such pairs

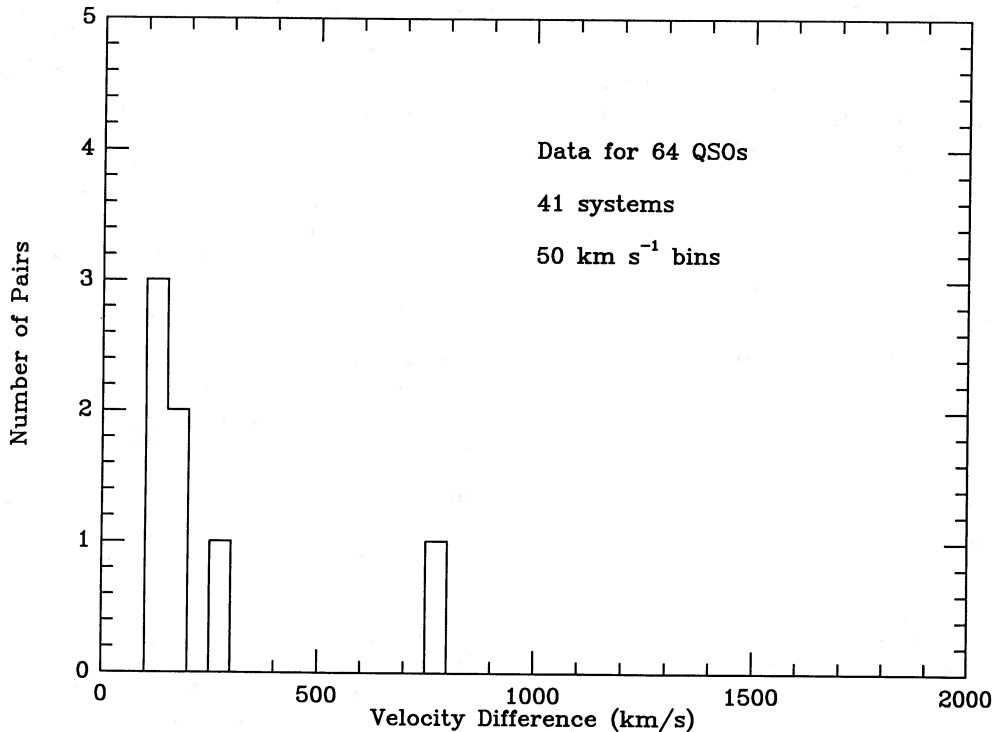


FIG. 4.—The two-point correlation for the Mg II absorption systems in sample MG 0

is only $P(n_{\text{pairs}} \geq 5) = 0.0007$. The two with the smallest values of Δv could be physical associations. The remaining three pairs among 12 systems have a Poisson probability of only 4.2%, which is uncomfortably low. As Tytler *et al.* pointed out, correlated ejection from the QSO would require velocities $\beta \sim 0.5$. On the other hand, if the apparent associations are due to large-scale clustering, then enormous scales (up to $600h^{-1}$ Mpc) must be involved. We do not find significant clustering on such large scales in our new data; as stated above, we find only four widely separated pairs and one widely separated triple out of 41 Mg II redshifts in the spectra of 64 QSOs. The fact that the number of Mg II redshifts per QSO spectrum matches a Poisson distribution to such a high degree (§ III) shows that these pairs are not statistically significant.

VI. SUMMARY AND DISCUSSION

We have analyzed the statistical properties of 40 absorption systems based on the Mg II doublet which were found in the spectra of 55 QSOs with emission redshifts in the range $1.8 < z_{\text{em}} < 3.56$ (see the companion paper by SBS). This sample was augmented by one Mg II system found in new spectra of nine QSOs with $z_{\text{em}} < 1.42$ and by published samples discussed by Tytler *et al.* (1987) and by LTW. Our new work has roughly doubled the available statistical sample of Mg II absorption redshifts. We summarize our conclusions as follows.

1. Many of our newly discovered Mg II systems fall at redshifts $z_{\text{abs}} < 0.7$, out to which there is a high probability of identifying the absorbing galaxy (Bergeron 1988).

2. We formed several unbiased samples of Mg II redshifts which are summarized in Tables 4 and 5. Table 4 uses different rest equivalent width cutoffs and augmentations with data from LTW and Tytler *et al.* (1987). Similar samples in Table 5 count pairs of absorption systems (in the same QSO) separated by $\Delta v < 1000 \text{ km s}^{-1}$ as one system.

3. The distribution of the number of Mg II absorption systems per QSO, suitably corrected for differences in the redshift coverage, fits a Poisson distribution to high accuracy (Bahcall-Peebles test 1; Table 6).

4. An application of the second Bahcall-Peebles test to sample P1 indicates that the absorbing objects are uniformly distributed along the line of sight to the QSO.

5. The preceding two results, together with Bergeron's (1988) high success rate in identifying a galaxy at the same redshift as Mg II absorption systems with $z_{\text{abs}} < 0.7$, provides overwhelming evidence for the cosmological origin of the systems.

6. We find that the number density of Mg II absorption redshifts increases significantly with redshift up to $z_{\text{abs}} \sim 1$, and then possibly flattens off in the range $1 < z_{\text{abs}} < 2$. It is likely that the rise in $N(z)$ at small redshifts is too steep to be compatible with a constant comoving density of absorbers if $q_0 = \frac{1}{2}$, but it is compatible if $q_0 = 0$.

7. The number density of Mg II systems with $W_0(2796) > 0.6 \text{ \AA}$ in the redshift range $1.3 < z_{\text{abs}} < 2.0$ is the same (within the errors) as the number density of C IV systems with $W_0(1548) > 0.6 \text{ \AA}$ in the same redshift range.

8. By combining the behavior of the Mg II systems at low redshift and the C IV systems (taken from SBS) at high redshifts, we suggest that the density of heavy element redshifts first rises up to $z \sim 1$, then flattens off, and finally declines beyond $z \sim 2.5$. This effect would most likely be interpreted as being due to the combined effects of cosmological expansion and the gradual formation of the heavy elements over cosmic time.

9. Contrary to earlier impressions (e.g., Perry, Burbidge, and Burbidge 1978), the density of Mg II absorption systems is statistically the same in the spectra of QSOs with high and low-emission redshifts.

10. The Mg II absorption systems are highly clustered on scales $\Delta v \leq 200 \text{ km s}^{-1}$. Both the high amplitude of the clustering and Bergeron's (1988) observations of a single, large galaxy as the absorber in a high fraction of cases leads us to conclude that the apparent clustering is due mostly to the relative motions of clouds within galaxies. Evidence exists for a much stronger correlation amplitude on velocity scales $100 \leq \Delta v \leq 200 \text{ km s}^{-1}$ for the Mg II systems than is observed for C IV, but this must be regarded as tentative until many more Mg II systems have been discovered. The clustering on scales $200 \leq \Delta v \leq 600 \text{ km s}^{-1}$ found by SBS for their C IV sample would not be detectable with our smaller sample of Mg II redshifts.

11. We do not confirm the evidence for significant Mg II clustering on very large scales found by Tytler *et al.* (1987).

In view of our finding that the number density of Mg II absorption systems is the same in high and low-redshift QSOs, it is clearly important to embark on a massive survey of low-redshift, bright QSOs in order to delineate the behavior of the $N(z)$ curve for $z_{\text{abs}} \leq 1.0$. As emphasized by SYBT, the slope of this curve at low redshifts in principle provides a powerful test

for q_0 . (The recent high success rate in identifying the absorbing galaxy out to $z \sim 0.7$ [Bergeron 1988] offers the promise that evolution in the absorbers can be corrected for.) Such a survey could also clarify the existence of clustering on very large scales, such as that found in the C IV systems (see § VIIg of SBS). LTW have made the important suggestion that the distinction between the "high" and "low" ionization systems results from differences in the optical depths of the absorbing cloud. Consequently, the ratio of the number densities of the two kinds of absorption system might be expected to evolve in redshift if it is the case that star formation in galaxies is a decreasing function of time. It should be possible, using the Hubble Space Telescope, to observe this effect directly by comparing the Mg II/C IV ratio as a function of redshift.

We thank John Fordham, Keith Shortridge, Dave Tennant, Juan Carrasco, Skip Staples, and John Henning for their help with the Palomar observations. The work was supported by NSF grants AST 84-16704 and AST 82-16544 to W. L. W. S. and by the UK Science and Engineering Research Council (A. B.).

REFERENCES

- Bahcall, J. N., and Peebles, P. J. E. 1969, *Ap. J. (Letters)*, **156**, L7.
 Bergeron, J. 1988, in *Large Scale Structure of the Universe*, ed. J. Audouze and A. S. Szalay (Dordrecht: Reidel), in press.
 Bergeron, J., D'Odorico, S., and Kunth, D. 1987, *Astr. Ap.*, **180**, 1.
 Blades, J. C. 1988, *QSO Absorption Lines: Probing the Universe*, ed. J. C. Blades, C. A. Norman, and D. A. Turnshek (Cambridge: Cambridge University Press), in press.
 Boksenberg, A., Carswell, R. F., and Sargent, W. L. W. 1979, *Ap. J.*, **227**, 370.
 Crotts, A. P. S. 1987, in *QSO Absorption Lines: Probing the Universe, A Collection of Poster Papers*, ed. J. C. Blades, C. A. Norman, and D. A. Turnshek (ST ScI Pub.), p. 119.
 Foltz, C. B., Weymann, R. J., Peterson, B. M., Sun, L., Malkan, M. H., and Chaffee, F. H. 1986, *Ap. J.*, **307**, 504.
 Lanzetta, K. M., Turnshek, D. A., and Wolfe, A. M. 1987, *Ap. J.*, **322**, 739 (LTW).
 Perry, J. J., Burbidge, E. M., and Burbidge, G. R. 1978, *Pub. A.S.P.*, **83**, 783.
 Sargent, W. L. W., Boksenberg, A., and Steidel, C. C. 1988, *Ap. J. Suppl.*, in press (SBS).
 Sargent, W. L. W., Young, P. J., Boksenberg, A., and Tytler, D. 1980, *Ap. J. Suppl.*, **42**, 41 (SYBT).
 Schechter, P. 1976, *Ap. J.*, **203**, 297.
 Tytler, D., Boksenberg, A., Sargent, W. L. W., Young, P. J., and Kunth, D. 1987, *Ap. J. Suppl.*, **64**, 667.
 Weymann, R. J., Williams, R. E., Peterson, B. M., and Turnshek, D. A. 1979, *Ap. J.*, **234**, 33.
 York, D. G., Dopita, M., Green, R. F., and Bechtold, J. 1986, *Ap. J.*, **311**, 610.
 Young, P., Sargent, W. L. W., and Boksenberg, A. 1982, *Ap. J. Suppl.*, **48**, 455 (YSB).

A. BOKSENBERG: Royal Greenwich Observatory, Herstmonceux Castle, Hailsham, East Sussex BN27 1RP, England

W. L. W. SARGENT and C. C. STEIDEL: Palomar Observatory, 105-24, California Institute of Technology, Pasadena, CA 91125